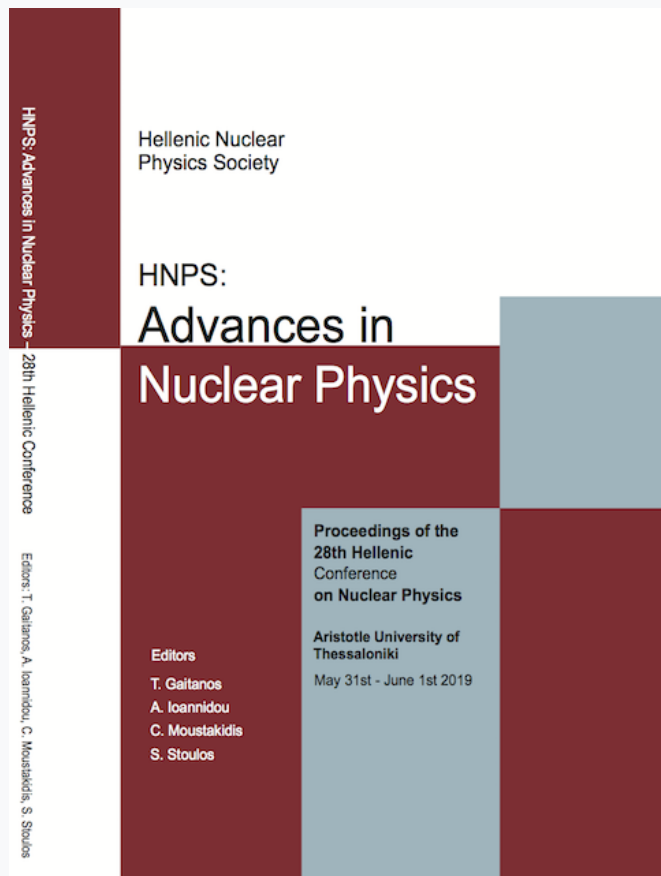


# HNPS Advances in Nuclear Physics

Vol 27 (2019)

HNPS2019



## Study of the $^{232}\text{Th}(\text{n},\text{f})$ Cross section at NCSR 'Demokritos' using Micromegas Detectors

*Sotirios Chasapoglou, A. Tsantiri, A. Kalamara, M. Kokkoris, V. Michalopoulou, A. Stamatopoulos, R. Vlastou, A. Lagoyannis, Z. Eleme, N. Patronis*

doi: [10.12681/hnps.2994](https://doi.org/10.12681/hnps.2994)

### To cite this article:

Chasapoglou, S., Tsantiri, A., Kalamara, A., Kokkoris, M., Michalopoulou, V., Stamatopoulos, A., Vlastou, R., Lagoyannis, A., Eleme, Z., & Patronis, N. (2020). Study of the  $^{232}\text{Th}(\text{n},\text{f})$  Cross section at NCSR 'Demokritos' using Micromegas Detectors. *HNPS Advances in Nuclear Physics*, 27, 106–111. <https://doi.org/10.12681/hnps.2994>

# Study of the $^{232}\text{Th}(\text{n},\text{f})$ Cross Section Using Micromegas Detectors at NCSR ‘Demokritos’

S. Chasapoglou<sup>1</sup>, A. Tsantiri<sup>1</sup>, A. Kalamara<sup>1</sup>, M. Kokkoris<sup>1</sup>, V. Michalopoulou<sup>1,2</sup>, A. Stamatopoulos<sup>1</sup>, R. Vlastou<sup>1</sup>, A. Lagoyannis<sup>3</sup>, Z. Eleme<sup>4</sup>, N. Patronis<sup>4</sup>

<sup>1</sup>Department of Physics, National Technical University of Athens, Zografou campus, 15780 Athens, Greece

<sup>2</sup>European Organization of Nuclear Research (CERN), Geneva, Switzerland

<sup>3</sup>Tandem Accelerator Laboratory, Institute of Nuclear Physics, N.C.S.R. ‘Demokritos’, Aghia Paraskevi, 15310 Athens, Greece

<sup>4</sup>Department of Physics, University of Ioannina, 45110 Ioannina, Greece

**Abstract** In the present work, the cross section of the  $^{232}\text{Th}(\text{n},\text{f})$  reaction has been measured relative to the  $^{238}\text{U}(\text{n},\text{f})$  reference reaction, at high neutron beam energies, with the use of the  $^3\text{H}(\text{d},\text{n})$  neutron production reaction. The experiment was performed at the 5.5 MV Tandem accelerator laboratory of N.C.S.R. ‘Demokritos’, using a Micromegas detector assembly. A variety of parasitic reactions take place during the neutron production, affecting the cross section measurements of the  $^{232}\text{Th}(\text{n},\text{f})$  reaction, due to its relatively low energy threshold. Thus emerges the need for a thorough characterization of the neutron flux impinging on the targets. The combined use of the NeuSDesc and MCNP5 Monte Carlo codes was implemented, for the reproduction of the neutron yield from the  $^3\text{H}(\text{d},\text{n})$  reaction, taking into consideration competing nuclear reactions (e.g. deuteron break up) along with neutron elastic and inelastic scattering with materials of the beam line, detector housing and experimental hall. Additional Monte-Carlo simulations were also performed coupling both GEF and FLUKA codes for the precise determination of the detector efficiency and the contribution of the  $\alpha$ -activity of the actinide samples in the fission fragment spectrum.

**Keywords** fission, cross section measurements, Monte Carlo simulations

Corresponding author: S. Chasapoglou (sot-ch@hotmail.com) | Published online: May 1st, 2020

## INTRODUCTION

The accurate knowledge of neutron induced fission cross section of actinides, such as  $^{232}\text{Th}$ , is of major importance when it comes to the optimization of the design of new generation nuclear reactors Generation-IV reactors and Accelerator Driven Systems (ADS) [1,2]). These reactors are proposed to use as fuel, what was considered to be nuclear waste in the past, utilizing fast neutron fission reactions. As an alternative option for nuclear fuel, the Th/U cycle is considered as a possible replacement of the conventional U/Pu fuel cycle in advanced nuclear reactors, with many advantages. The most important is that ADS systems produce the fissile actinides  $^{233}\text{U}$  or  $^{239}\text{Pu}$  from natural Th ( $^{232}\text{Th}$  100%) and U ( $^{238}\text{U}$  99.3%) that are abundant in nature. The Th/U fuel cycle is also important in reducing the amount of high level transuranic waste and is inherently proliferation resistant, since the isotopes involved are not utilized for weapons production. Feasibility and sensitivity studies for the design of this new generation of nuclear reactors, which are planned to make sustainable use of fuel resources and to minimize nuclear waste, require the knowledge of accurate and consistent cross sections of all the involved reactions. However, severe discrepancies exist in the evaluations and the cross section data in literature, thus, new accurate data are required in order to reduce the uncertainties in the design of the proposed systems. The available datasets for the  $^{232}\text{Th}(\text{n},\text{f})$  case are either few (at intermediate neutron energies), or discrepant (with differences reaching 27% for high neutron energies), consequently leading to problematic evaluations. In this scope, the aim of the present work was the measurement of the  $^{232}\text{Th}(\text{n},\text{f})$  cross section at 14.8, 16.5 and 17.8 MeV neutron energies.



Licensed under a Creative Commons Attribution-NonCommercial-NoDerivatives 4.0 International License.

## EXPERIMENTAL DETAILS

### Neutron facility and detection system

The experiment was performed at the 5.5 MV Tandem Van de Graaff Accelerator, at N.C.S.R. “Demokritos”. The neutron beams were produced at high energies, 14.8, 16.5 and 17.8 MeV, by means of the  $^3\text{H}(\text{d}, \text{n})^4\text{He}$  reaction. The 0.2–0.5  $\mu\text{A}$  deuterium beam impinged on a solid Ti-tritiated target of 373 GBq activity consisted of a 2.1  $\text{mg}/\text{cm}^2$  Ti-T layer (25.4 mm in diameter) on a 1mm thick Cu backing (28.5 mm in diameter). A 10  $\mu\text{m}$  molybdenum foil (entrance foil) was placed in front of the Ti-tritiated target. The reason for this is that the initial acceleration of deuterons at slightly higher energies than the desired ones (as measured in the middle of the Ti-T solid target), ensures a higher intensity of the deuteron beam, leading to a larger neutron production, which in turn results in better counting statistics in the recorded fission yield spectra, at the expense of course of a slight increase in the energy straggling.

The actinide samples were placed along with the Micromegas detectors [3], in a cylindrical aluminum chamber, filled with a circulating Ar:CO<sub>2</sub> (80:20) gas mixture at atmospheric pressure. In Fig. 1, both of the aforementioned neutron producing target and target-detector assembly, are presented.

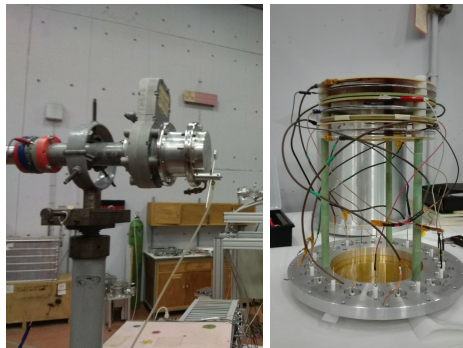


**Figure 1.** The neutron producing target (left) and the target-detector assembly (right)

### Actinide samples

The actinide samples used in the present experiment, were thin disks of ~5.2 cm in diameter deposited on a 100  $\mu\text{m}$  Al backing produced via the painting technique at the IPPE (Obninsk) and JINR (Dubna). Apart from the  $^{232}\text{Th}$  actinide sample, a  $^{238}\text{U}$  sample was used as reference target and a  $^{235}\text{U}$  sample as a sensitive detector for the low energy parasitic neutrons due to its high fission cross section in the low energy region. During the irradiations, Al masks (0.6 mm in thickness, 5.0 cm in diameter) were placed in front of the targets to achieve the desired angular acceptance of the neutron beam with respect to its axis, in order to minimize the energy uncertainty during the irradiations, while ensuring adequate statistics.

The accurate determination of the number of nuclei in all samples involved in a cross section measurement is of crucial importance. This determination was made possible via  $\alpha$ -spectroscopy measurements, using a Silicon Surface Barrier (SSB) detector at the Nuclear Physics Laboratory of the National Technical University of Athens. The silicon detector (6.2 cm in diameter and 60  $\mu\text{m}$  in thickness) was placed in a vacuum ( $\sim 10^{-4}$  atm) chamber, at a distance of 0.1 cm from each actinide sample. The estimation of the solid angle between the detector and the sample, which is the main source of a systematic uncertainty in the final results, was carried out via the SACALC [4] Monte Carlo code. A typical spectrum of the  $^{232}\text{Th}$  sample is shown in Fig. 2. The determination of the number of nuclei

in the sample was derived with the use of the expression:

$$N = C_\Omega \cdot \frac{4\pi}{\Omega} \cdot \frac{t_{1/2}}{\ln 2}$$

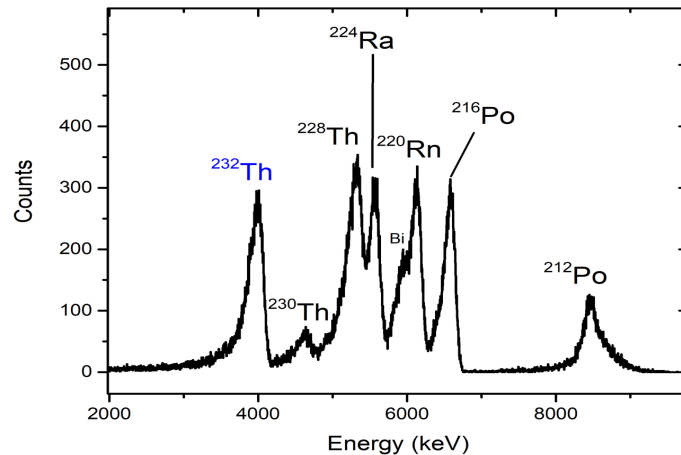


**Figure 2.** A typical spectrum of the  $\alpha$ -activity of the  $^{232}\text{Th}$  sample. Along with the peak produced by the  $\alpha$ -decay of  $^{232}\text{Th}$ , some other peaks also appear in the spectrum, corresponding to different isotopes attributed to the decay chain of  $^{232}\text{Th}$ .

Where:

- $N$  is the calculated number of nuclei of the isotope in question (in this case  $^{232}\text{Th}$ );
- $C_\Omega$  are the  $\alpha$ -particles, measured by the silicon detector, per second;
- $\Omega$  is the solid angle between the actinide target and the silicon detector;
- $t_{1/2}$  is the half life of the actinide target in seconds.

All the actinide samples  $^{232}\text{Th}$ ,  $^{238}\text{U}$  and  $^{235}\text{U}$ , used in the present work, have been characterized with this method for the accurate determination of their contents.

## MONTE CARLO SIMULATIONS

The simulation of the produced neutron spectra was accomplished via the combined use of NeuSDesc [5] and MCNP5 [6] Monte Carlo codes. Given the necessary input (such as the type of reaction, ion energy, entrance foil thickness etc.), the NeuSDesc code produces as output a detailed description of the neutron beam from the D-T reaction. The energy loss of the deuteron beam in the Mo foils is taken into account via SRIM (Stopping and Range of Ions in Matter) [7] calculations. This output can be used as an input source (sdef card) in the more detailed MCNP5 simulations, which include all the detailed geometry of the flange with the Ti-T target and the chamber with the target-detector assembly. The results of these simulations at 14.8, 16.5 and 17.8 MeV, are given in Fig. 3.

Auxiliary Monte Carlo simulations were also performed with the combined use of GEF and FLUKA codes, for the accurate determination of the detector efficiencies and were found to be 99.99% of the emitted fission fragments.

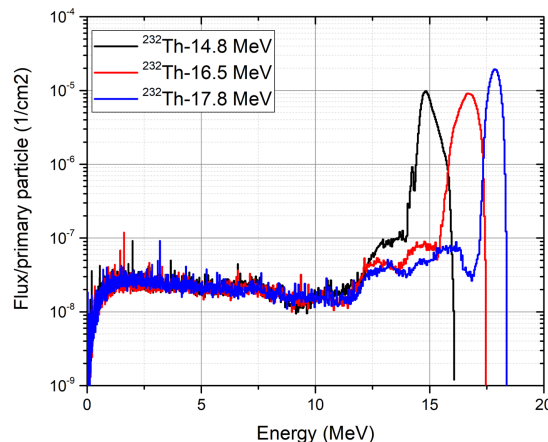


**Figure 3.** Unnormalized neutron flux for the three different irradiations at high neutron energies, as obtained by the NeuSDesc and MCNP5 codes. Apart from the main energy peak in each nominal neutron energy, a low energy parasitic tail also appears, mainly because of the neutron scattering.

## DATA ANALYSIS

The cross section for the  $^{232}\text{Th}(\text{n},\text{f})$  reaction is given by the expression:

$$\sigma_{^{232}\text{Th}} = \frac{(Y \cdot f_{amp} \cdot f_{abs} \cdot f_{DT} \cdot f_{scat} \cdot f_{line})_{^{232}\text{Th}}}{(Y \cdot f_{amp} \cdot f_{abs} \cdot f_{DT} \cdot f_{scat} \cdot f_{line})_{^{238}\text{U}}} \cdot \frac{N_{^{238}\text{U}}}{N_{^{232}\text{Th}}} \cdot \frac{\Phi_{^{238}\text{U}}}{\Phi_{^{232}\text{Th}}} \cdot \sigma_{^{238}\text{U}}$$

where

- $Y$  is the fission yield recorded by the Micromegas detectors and corrected for: the amplitude threshold introduced in the analysis ( $f_{amp}$ ), the self absorption of the  $\alpha$ -particles in the actinide sample ( $f_{abs}$ ), the dead time ( $f_{DT}$ ), and the contribution from low energy parasitic neutrons in the fission yield, stemming from respective parasitic reactions such as neutron scattering ( $f_{scat}$ ) and  $(d, n)$  reactions within the beam line ( $f_{line}$ );
- $N$  is the number of nuclei in the actinide samples;
- $\Phi$  is the neutron fluence on each sample, expressed in  $\text{neutrons}/\text{cm}^2$ , corresponding to the main energy peak;
- $\sigma_{^{238}\text{U}}$  is the cross section of the reference target obtained from evaluation libraries.

### Fission yield and corrections

In Fig. 4 a typical fission spectrum obtained by a Micromegas detector for the  $^{235}\text{U}$  case is presented. The  $\alpha$ -particles from the  $\alpha$ -activity of the actinide sample are of lower energy, thus they are recorded on the left hand side of the spectrum, while the opposite happens for the much more energetic fission fragments. An amplitude threshold must then be introduced in the analysis, to separate the two areas. Some fission fragments though, emitted at large angles, deposit a comparable amount of energy to the one of  $\alpha$ -particles, thus mixing with the  $\alpha$ -background. The estimation of the percentage of fission fragments “lost” under the  $\alpha$ -background ( $f_{amp}$ ), was made possible via the coupled use of the GEF and FLUKA codes. It is noted that the same simulation was used for the estimation of the self absorption of fission fragments in the actinide sample ( $f_{abs}$ ).

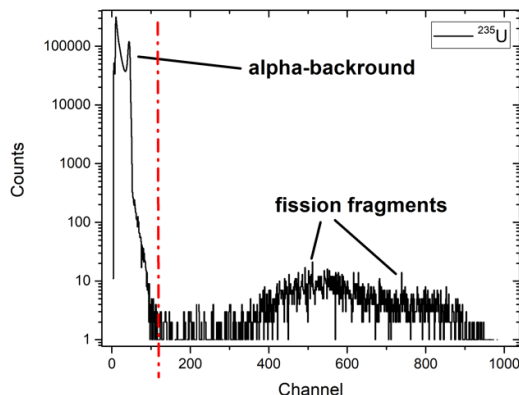


**Figure 4.** A typical fission spectrum obtained by the Micromegas detector for the  $^{235}\text{U}$  case at 16.5 MeV incident neutron energy. The red dotted line represents the amplitude threshold introduced in the analysis, separating the  $\alpha$ -background from the fission fragments.

The dead time correction in the fission spectrum is simply given by the expression:

$$f_{DT} = \frac{\text{Live time}}{\text{Real time}}$$

where live and real time refer to the respective times of the recorded spectrum.

The estimation of the contribution of the scattered parasitic neutrons is made possible via the combined use of NeuSDesc and MCNP5 Monte Carlo codes, the output of which is presented in Fig. 3. Given this simulated neutron fluence and the evaluated cross section of the  $^{238}\text{U}$  reference target, the reaction rate can be calculated by multiplying the fission cross section with the simulated neutron fluence, following the methodology described in detail in [8]. The ratio of the integrated reaction rate corresponding to the main neutron beam to the total integrated reaction rate, provides the contribution  $f_{scat}$  of the scattered parasitic neutrons to the recorded fission yield.

$$f_{scat} = \frac{[\sum \sigma(E) \cdot \Phi(E)]_{\text{main beam}}}{[\sum \sigma(E) \cdot \Phi(E)]_{\text{total}}}$$

where the subscript “*total*” refers to the total energy spectrum, while the “*main beam*” one, refers to the energy spectrum of the main beam. The  $^{238}\text{U}$  target was practically used as a reference sample, since it reveals the same energy behavior as the  $^{232}\text{Th}$  fission cross section, while the  $^{235}\text{U}$  is much more sensitive to the low energy parasitic neutrons and was only used as an indication for the existence of such neutrons.

Finally, the contribution of the parasitic neutrons stemming from the respective parasitic reactions within the beam line materials ( $f_{line}$ ), is estimated experimentally by replacing the Ti/T target by a Cu foil, so that any fission fragments recorded by the Micromegas detectors can be attributed to parasitic reactions taking place within the beam line.

## RESULTS

The preliminary results for the neutron induced fission cross section values of the  $^{232}\text{Th}(n,f)$  reaction obtained using the aforementioned analysis methodology are shown in Fig. 5, along with previous data and the existing evaluation libraries [9-11].

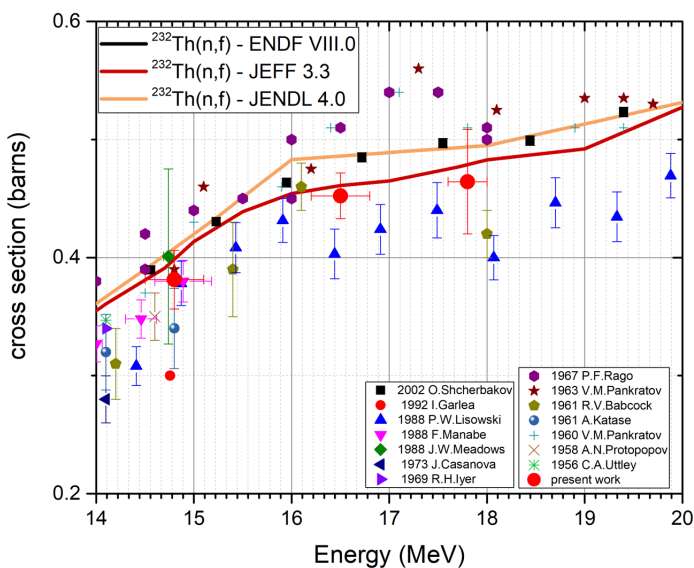


**Figure 5.** The results for the  $^{232}\text{Th}(n,f)$  cross section measurement.

The data seem to be in good agreement with the existing experimental data of Manabe [12] and Lisowski [13] as well as with the ENDF VIII.0 evaluation library within the statistical error of the measurements. Further measurements are planned in the near future at intermediate energies, implementing the  $^2\text{H}(\text{d},\text{n})$  reaction.

## Acknowledgments

The authors would like to acknowledge the assistance of the Accelerator Staff at NCSR “Demokritos”.

## References

- [1] NEA, Accelerator-driven Systems (ADS) and Fast Reactors (FR) in advanced nuclear fuel Cycles, Technical Report (Nuclear Energy Agency of the OECD, NEA, 2002).
- [2] <https://www.gen-4.org>, Gen-IV International Forum.
- [3] Y. Giomataris, Nucl. Instrum. Methods A 419, 239 (1998).
- [4] R. Whitcher, SACALC3, <https://sites.google.com/site/averagesolidangle2/dow/sacalc3>
- [5] J.F. Ziegler, Nucl. Instrum. Methods B 219, 1027 (2004)
- [6] L. Waters et al., AIP Conf. Proc. 896, 81 (2007).
- [7] J. Ziegler, Stopping and range of ions in matter, SRIM 2013, url: <http://www.srim.org>.
- [8] A. Stamatopoulos et al. Eur. Phys. J. A 54.1, 7 (2018), doi: 10.1140/epja/i2018-12429-2
- [9] ENDF, doi: 10.1016/j.nds.2011.11.002
- [10] JEFF 3.3, doi: 10.1016/j.nds.2018.02.002
- [11] JENDL 4.0, doi: 10.1080/18811248.2011.9711675
- [12] F. Manabe et al. Fac. of Engineering, Tohoku Univ. Tech. Report 52, 97 (1988).
- [13] P.W. Lisowski et al., Conf. on Nucl. Data For Sci. and Technol. 97 (1988).